Electric Analog of Three-Dimensional Flow to Wells and Its Application to Unconfined Aquifers

GEOLOGICAL SURVEY WATER-SUPPLY PAPER 1536-H

Electric Analog of Three-Dimensional Flow to Wells and Its Application to Unconfined Aquifers

By ROBERT W. STALLMAN

GROUND-WATER HYDRAULICS

GEOLOGICAL SURVEY WATER-SUPPLY PAPER 1536-H

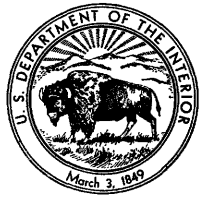

UNITED STATES GOVERNMENT PRINTING OFFICE, WASHINGTON : 1963

UNITED STATES DEPARTMENT OF THE INTERIOR

STEWART L. UDALL, *Secretary*

GEOLOGICAL SURVEY

Thomas B. Nolan, *Director*

For sale by the Superintendent of Documents, U.S. Government Printing Office
Washington 25, D.C.

CONTENTS

ILLUSTRATIONS

TABLES

ELECTRIC ANALOG OF THREE-DIMENSIONAL FLOW TO WELLS AND ITS APPLICATION TO UNCONFINED AQUIFERS

By ROBERT W. STALLMAN

ABSTRACT

Electric-analog design criteria are established from the differential equations of ground-water flow for analyzing pumping-test data. A convenient analog design was obtained by transforming the cylindrical equation of flow to a rectilinear form. The design criteria were applied in the construction of an electric analog, which was used for studying pumping-test data collected near Grand Island, Nebr.

Data analysis indicated (1) vertical flow components near pumping wells in unconfined aquifers may be much more significant in the control of water-table decline than radial flow components for as much as a day of pumping; (2) the specific yield during the first few minutes of pumping appears to be a very small fraction of that observed after pumping for more than 1 day; and (3) estimates of specific yield made from model studies seem much more sensitive to variations in assumed flow conditions than are estimates of permeability.

Analysis of pumping-test data where vertical flow components are important requires that the degree of anisotropy be known. A procedure for computing anisotropy directly from drawdowns observed at five points was developed.

Results obtained in the analog study emphasize the futility of calculating unconfined aquifer properties from pumping tests of short duration by means of equations based on the assumptions that vertical flow components are negligible and specific yield is constant.

INTRODUCTION

Most analytical expressions used in analyzing discharging-well types of aquifer tests are based on the assumption that components of vertical flow are negligible. Usually artesian, or confined, flow to wells is adequately defined by this assumption. Methodology associated with such analysis has been described by Wenzel (1942), Ferris (1949), Jacob (1950), and Ferris and others (1962). Flow to wells in unconfined aquifers, on the other hand, is more often highly dependent on the velocity components parallel with the well axis. Boulton (1954) has developed an analytical solution of nonsteady flow to a fully penetrating well; and, more recently, Kirkham (1959) has presented

a means for analyzing steady flow to partially penetrating wells, both of which account for these vertical flow components.

In field testing, wells generally penetrate only a part of the aquifer thickness and are operated for testing purposes for such a short period of time that flow is nonsteady during the test. The investigations individually reported by Boulton and Kirkham are significant advances in test analysis, but a need exists for an analytical procedure that in effect combines their respective contributions. Specifically, therefore, a method of analyzing nonsteady flow to a partially penetrating well, treating both radial and vertical velocity components, is required.

The complexity of the analyses described by Boulton (1954) and Kirkham (1959) leads one to the belief that any expression obtained from a combination of the boundary systems used by each may be impractical for general use in hydrologic investigations. With this prospect in view, some technique other than the calculus appears to be desirable in developing methods of test analysis.

This report describes the design and use of an electrical model of the field of flow in the vicinity of a discharging partially penetrating well. The model, as devised, is a mechanism for solving the finite-difference approximations of the differential equations of flow. The interrelations among the aquifer and model characteristics are discussed and the model is applied to a particular analysis of selected aquifer-test data. Finally, the general utility of the analog for pumping-test analysis is outlined.

EQUATIONS OF FLOW

Confined flow and unconfined flow are illustrated in figure 56. Figure 56*A* represents the classic concept of nonsteady artesian flow to a well as defined by Theis (1935). If the aquifer can be considered homogeneous and isotropic, the drawdown, s, signifying the change in head due to a change in rate of pumping, at each point follows the relation:

$$\frac{\partial^2 s}{\partial r^2}+\frac{1}{r}\frac{\partial s}{\partial r}=\frac{S'}{P}\frac{\partial s}{\partial t}, \tag{1}$$

where r is the distance from the centerline of the pumping well to a point at which s is observed; S' is the storage coefficient per unit volume of aquifer; P is the permeability of the aquifer material; and t is the elapsed time since a change in rate of pumping occurred. In the flow system characterized by figure 56*A* and equation 1, the vertical flow components have been assumed to be negligible. This permits expression of the ratio S'/P in terms of the aquifer characteristics as S/T, where S is the aquifer storage coefficient (approxi-

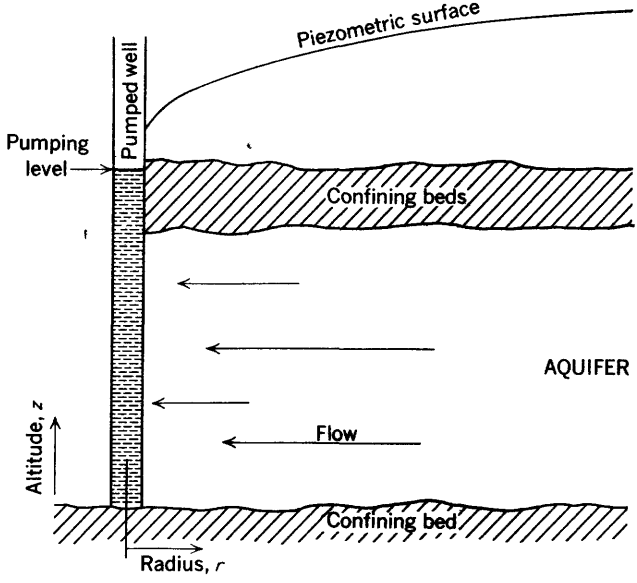

A. Confined aquifer

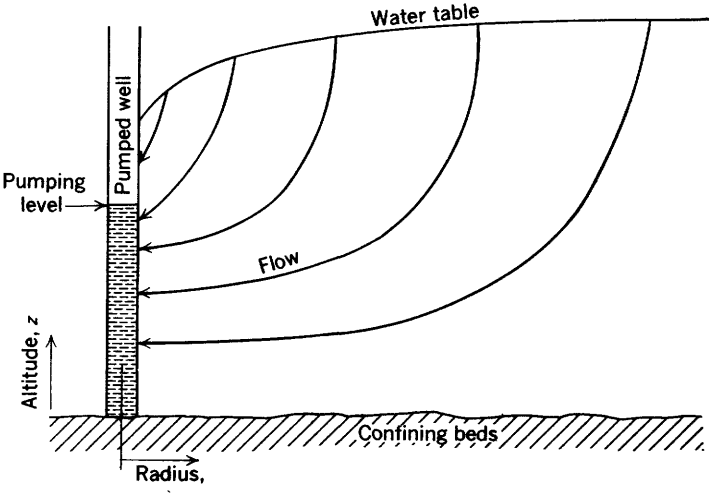

B. Unconfined aquifer

FIGURE 56.—Schematic of instantaneous paths of flow in the vicinity of a pumped well. *A*, Confined aquifer; *B*, Unconfined aquifer.

mately equal to the aquifer thickness, m, times S'), and T is the aquifer transmissibility (m times P), as defined by Wenzel (1942). Thus equation 1, rewritten for the total aquifer thickness, is

$$\frac{\partial^2 s}{\partial r^2}+\frac{1}{r}\frac{\partial s}{\partial r}=\frac{S}{T}\frac{\partial s}{\partial t}. \tag{2}$$

Equation 2 follows also from the equation of continuity applied to the aquifer thickness and from the assumptions: (1) that the aquifer is homogeneous and isotropic; (2) that flow obeys Darcy's law; and (3) that discrete amounts of water are released from storage, because water expands and the aquifer contracts as pressure is reduced locally in the flow field.

In the flow system illustrated in figure 56*B*, the expression for the drawdown at any point between the water table and lower confining bed may be written in the form

$$P_r\left[\frac{\partial^2 s}{\partial r^2}+\frac{1}{r}\frac{\partial s}{\partial r}\right]+P_z\frac{\partial^2 s}{\partial z^2}=S'\frac{\partial s}{\partial t}, \tag{3}$$

where P_r is the permeability along the r axis and P_z is the permeability along the z axis. Equation 3 differs from equation 1 only in that the effects of vertical flow components are included through addition of the term $\frac{\partial^2 s}{\partial z^2}$ and that effects of stratification on directional permeability are recognized. The complete interrelations among s, r, z, and t depend on equation 3 and on the boundary conditions at the well screen and along the free surface. Boulton (1954, p. 568) described the boundary condition at the free surface, whence it can be shown that:

$$S_y\frac{\partial s}{\partial t}=P_r\left(\frac{\partial s}{\partial r}\right)^2+P_z\left[\left(\frac{\partial s}{\partial z}\right)^2-\frac{\partial s}{\partial z}\right], \tag{4}$$

where S_y is the specific yield (Ferris and others, 1962) and it is assumed that no recharge or discharge crosses the water table. Equation 4 applies along the free surface only, and S_y can be considered a variable in space or time.

In unconfined systems, the total effect on the relation between drawdown and time caused by the storage changes due to a change in the water-table position are generally of a much greater magnitude than those resulting from decompression of the water below the water table. Thus for the flow system shown on figure 56*B*, drawdown may be defined in approximate form by

$$P_r\left[\frac{\partial^2 s}{\partial r^2}+\frac{1}{r}\frac{\partial s}{\partial r}\right]+P_z\frac{\partial^2 s}{\partial z^2}=0 \tag{5}$$

at all points between the water table and the confining bed for the boundary conditions that are considered.

The assumption $S' \frac{\partial s}{\partial t}=0$ appears to be a valid approximation for the system analyzed later in this report. However, it must be recognized that under certain conditions—including very low pumping rates, nonhomogeneity, low values of the ratio S_y/P_z, or exceptionally thick aquifers—the effects on water levels caused by release from internal storage may indeed be significant. Equation 5 seems to be a satisfactory approximation of the aquifer system analyzed in detail later in this report. Its use simplified the analytical solution developed by Boulton (1954) and will also simplify analog construction. However, use of the complete form, equation 3, offers no barrier to model design or analysis.

FINITE-DIFFERENCE APPROXIMATIONS OF FLOW EQUATIONS

An electric analog is envisioned in which each component is the physical counterpart of a given block of aquifer material. The analog is to represent all the aquifer material between the water table and the confining bed, from the pumping-well radius r_w out to some external radius r_e where the effects on water levels caused by pumping are negligible. In order to devise such an analog, the differential notation employed in stating the flow problem is expanded, so that the flow equation finally used as the basis for model design relates specifically to finite blocks of the flow field rather than to infinitesimal volumes. This might be accomplished by writing equation 5 in terms of finite differences directly, but the result would lead to an unnecessarily complicated model design. Consequently, equation 5 is transformed as suggested by Southwell (1946, p. 44).

Letting $\xi=\log r$, equation 5 is rewritten

$$\frac{P_r}{P_z}\frac{1}{r^2}\frac{\partial^2 s}{\partial \xi^2}+\frac{\partial^2 s}{\partial z^2}=0. \tag{6}$$

The finite-difference forms of the terms in equation 6 (Southwell, 1946, p. 16) used are

$$\frac{P_r}{P_z}\frac{1}{r^2}\frac{\partial^2 s}{\partial \xi^2}\simeq\frac{P_r}{P_z}\left(\frac{1}{r_n\Delta\xi}\right)^2(s_{n-1}-2s_n+s_{n+1}) \tag{7}$$

and

$$\frac{\partial^2 s}{\partial z^2}\simeq\left(\frac{1}{\Delta z}\right)^2(s_{p-1}-2s_p+s_{p+1}). \tag{8}$$

The complete finite-difference form of equation 6 at any point (p, n) corresponding with (z, ξ) is obtained by substitution of equations 7 and 8, from which

$$s_{n-1}-2s_n+s_{n+1}+\frac{P_z}{P_r}\left(\frac{r_n\Delta\xi}{\Delta z}\right)^2(s_{p-1}-2s_p+s_{p+1})\simeq 0. \tag{9}$$

The finite lengths Δz and $\Delta\xi$ and the subscript notation of equations 7, 8, and 9 are identified on figure 57. Equation 9 must be satisfied at

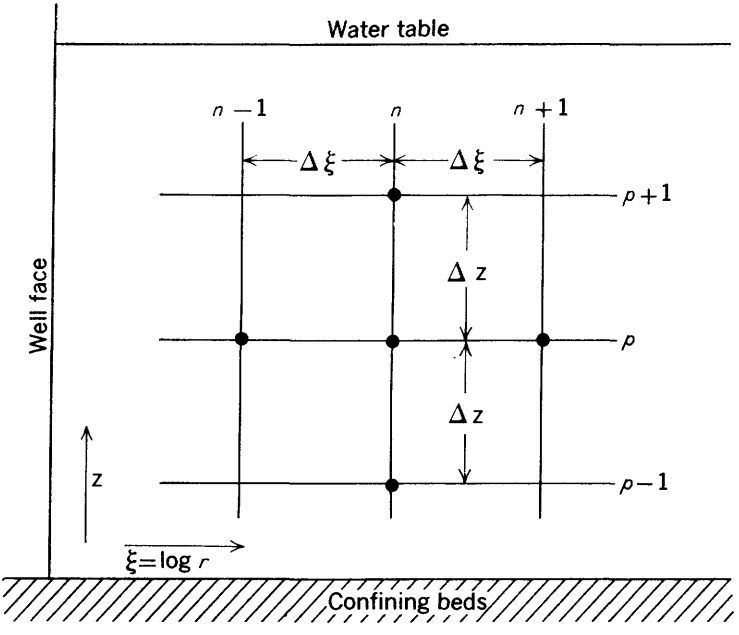

FIGURE 57.—Finite-difference grid in a field of radial flow.

each point in the finite representation of the field of flow. In accordance with figure 57 and the basis for equation 9, these points are illustrated schematically in figure 58. The interval $\Delta\xi$ is constant between all grid lines parallel with the z axis, and the interval $\Delta\xi$ is constant between all grid lines parallel with the ξ axis. By definition

$$\Delta\xi=\xi_{n+1}-\xi_n=\xi_n-\xi_{n-1}=\log\frac{r_{n+1}}{r_n}=\log\frac{r_n}{r_{n-1}}. \tag{10}$$

The accuracy with which the finite-difference grid represents the flow field increases with the number of grid intersections employed to represent a given region of the flow field. For a two-dimensional grid like that shown on figure 3, satisfactory accuracy might be achieved by

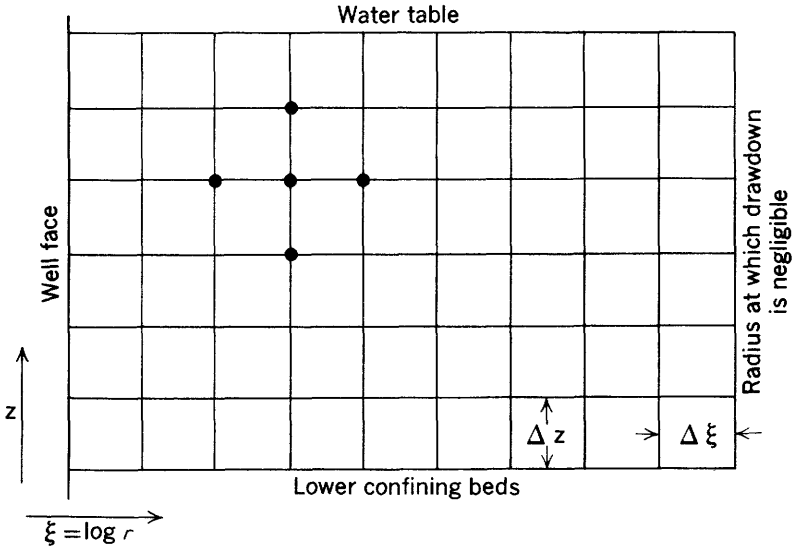

FIGURE 58.—Finite-grid subdivision of the field of radial flow.

a minimum of about 100 grid intersections spread through the area of significant flow. In effect, such a grid would represent 100 equations like equation 9, containing 100 unknown values of s. Such a set of simultaneous equations could be written and solved directly to obtain the drawdown distribution for specified boundary conditions, but the electric analog appears to be a more convenient approach to solution.

RESISTANCE ANALOG

A junction at which four resistors terminate, with the resistances oriented along the ξ' and z' axes, is shown on figure 59. Assuming there is a voltage distribution of some form arbitrarily established at the extreme ends of the resistances, the current to the junction (p', n') is given by Kirkoff's law as

$$(e_{n'-1}-2e_{n'}+e_{n'+1})/R_{\xi'}+(e_{p'-1}-2e_{p'}+e_{p'+1})/R_{z'}=0, \qquad (11)$$

where e is the voltage at the point indicated by the subscript; $R_{\xi'}$ is the resistance of the elements between $n'-1$ and n' and between n' and $n'+1$; and $R_{z'}$ is the resistance of the elements between $p'-1$ and p' and between p' and $p'+1$.

The analogy between the forms of equations 9 and 11 is obvious, and apparently the junction shown on figure 59 may be adopted as an analogy of the condition expressed by equation 9 if e is taken proportional to s, and if

$$R_{z'}/R_{\xi'}=P_r(\Delta z)^2/P_z(r_n\Delta\xi)^2. \qquad (12)$$

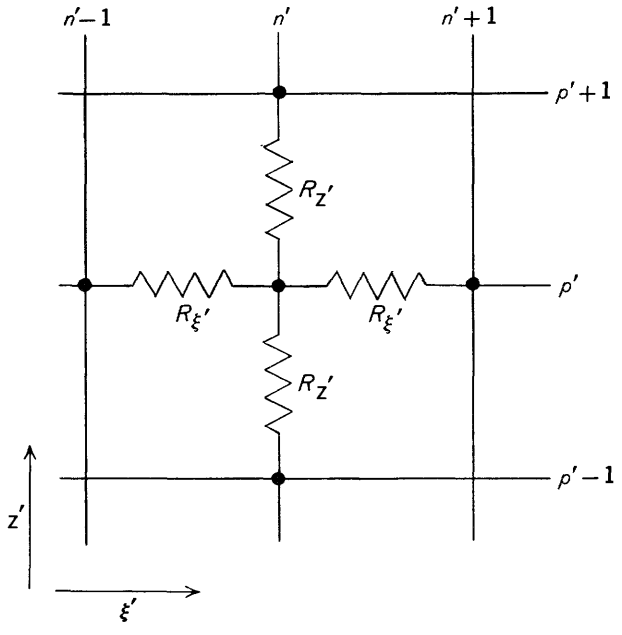

FIGURE 59.—Junction of four resistance elements.

From the latter relations, a grid of resistance elements may be devised to fit between the grid intersections shown on figure 58. The resistor grid thus established is analogous to the finite-difference equations of the flow field internal to the boundaries.

Along the base of the aquifer the vertical flow component is zero. The spatial distribution of the grid intersections with respect to the lower boundary and the equivalent resistor grid are shown on figure 60. The grid lines in the aquifer section have been located arbitrarily so that one line along the ξ axis lies directly on the contact between the aquifer and the confining bed. Equation 9 applies at every grid intersection lying along the boundary, with the added condition that $(s_{p-1}-s_p)/\Delta z=0$. The latter is derived easily from the requirement that the vertical gradient $\partial s/\partial z=0$ along the confining bed. Part of the resistor grid along the lower boundary representing the aquifer segment of figure 60*A* is shown on figure 60*B*. Maintaining the electrical analogy assumed for the interior grid intersections requires that $e_{p'-1}-e_{p'}=0$. In the electric analog, this condition may be established by making all values of $R_{z'}$ beneath the contact equal to infinity. This is accomplished by simply terminating the resistor grid in the z' axis directly beneath the analogous contact between the aquifer and confining bed.

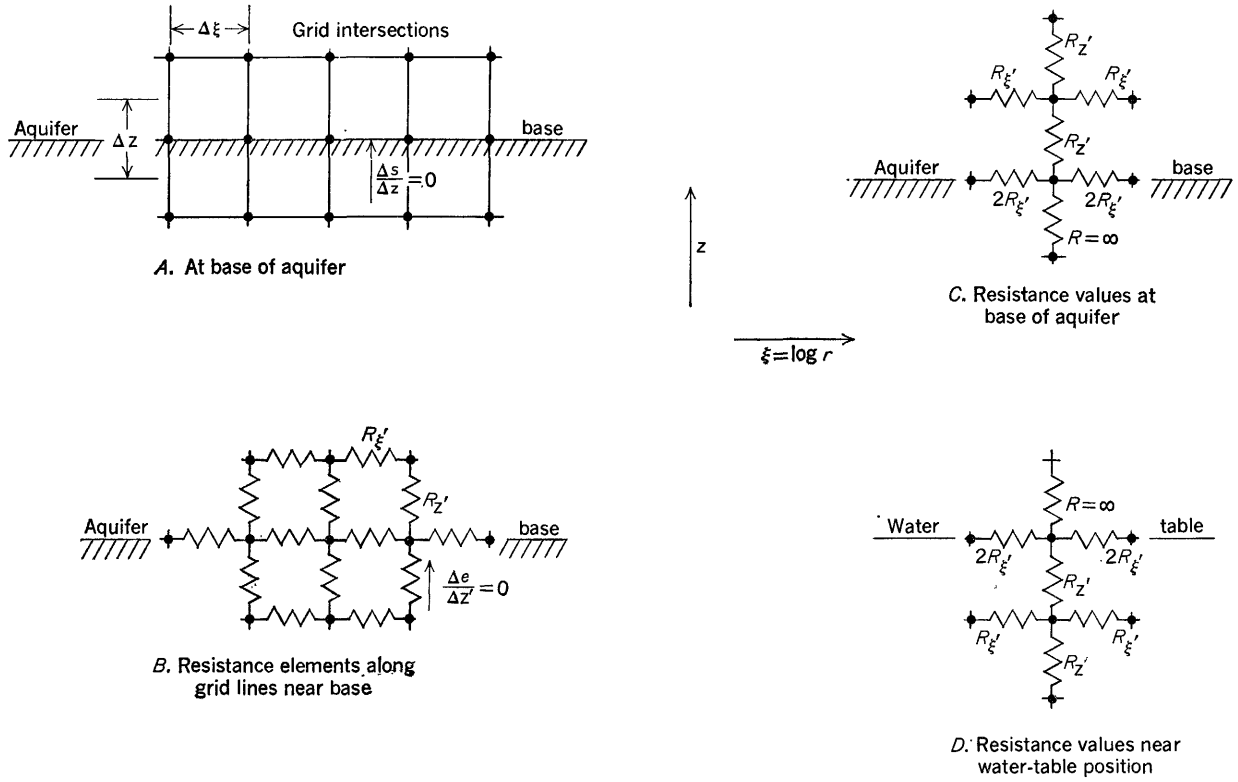

FIGURE 60.—Finite grid and resistance elements representing boundary regions. *A*, At base of aquifer; *B*, Resistance elements along grid lines near base; *C*, Resistance values at base of aquifer; *D*, Resistance values near water-table position.

Comparison of figure 60*A* with 60*B* shows that $R_{\xi'}$ along the contact represents an aquifer thickness of Δz, which, in effect, extends below the contact position by an amount $\Delta z/2$. Some adjustment in $R_{\xi'}$ values along the boundaries must be made to account for the smaller flow segment they represent, as compared with the areas represented at interior grid intersections. According to the view held by Southwell (1946, p. 77), grid spacing along the boundary represents a prototype section with twice the resistance between comparable grid points in the interior of the flow field. Thus the boundary resistors should have twice the resistance of those in the interior at comparable ξ' values, as indicated on figure 60*C*. If the water-table decline is small compared with Δz, the resistor grid at points along the water table will have the same relative design, as indicated on figure 60*D*.

The effect of terminating the grid at large values of r will be discussed later. To this point, sufficient conditions have been established to identify the analogic resistance values as a function of ξ and z.

APPROACH TO PUMPING-TEST ANALYSIS

The flow conditions in the vicinity of a partially penetrating pumped well in an unconfined aquifer, shortly after pumping begins, are shown schematically on figure 61. It is assumed that the pumping level is held constant as a function of time. Initially the water table is everywhere horizontal. Before water levels begin to decline along the surface of the saturated zone, a head gradient between the water

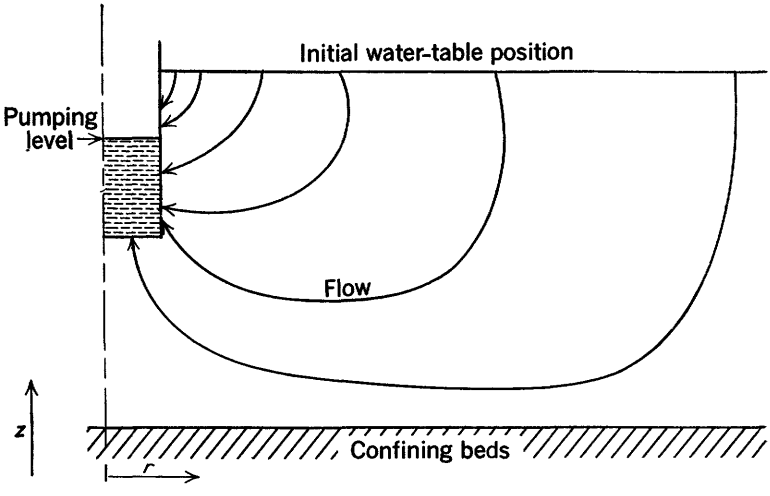

FIGURE 61.—Initial flow conditions near a partially penetrating pumped well in an unconfined aquifer.

table and well face is produced in response to the reduced water level in the pumped well. Along the water table, this gradient is initially directed downward and perpendicular to the water table. The downward motion at all points along the water table in response to this gradient—as a function of the aquifer permeability, specific yield, and time—is defined by equation 4. For a short period of time after pumping begins, the water table may be considered virtually horizontal over most of its area. Also, over most of the water table the term $\partial s/\partial z$ will be much larger than the term $(\partial s/\partial z)^2$. Therefore, equation 4 may be simplified to

$$S_y \frac{\partial s}{\partial t} = -P_z \frac{\partial s}{\partial z}. \tag{13}$$

Both sides of equation 13 simply represent the velocity of the water-table decline parallel to the z axis.

All pumpage at the well is assumed to be derived from the downward movement of the water table and therefore the discharge rate, Q, at the well may be expressed as

$$Q = -P_z \int_{r_w}^{r_e} (\partial s/\partial z)_r 2\pi r dr, \tag{14}$$

where $(\partial s/\partial z)_r$ is the vertical gradient at the water table at radius r. The integral term of equation 14 may be evaluated easily by graphical analysis of an electric-model study, and Q is observed in the field test. Thus P_z may be obtained directly from use of equation 14. The rate of change of the water-table position is observed at a given distance from the pumped well, from which an estimate of $\partial s/\partial t$ is available; the value of $(\partial s/\partial z)_r$ may be estimated at that point from the model analysis, and S_y computed from these data may be put in equation 13. This, of course, presumes that the ratio P_r/P_z is known from other sources of information and that the model was constructed and analyzed with full recognition of this ratio.

DESIGN AND CONSTRUCTION OF THE MODEL

A particular model design was selected to illustrate the method of analyzing pumping tests described in this report. The model criteria discussed earlier and the shape of the flow system to be analyzed govern the selection of resistance elements to be assembled in the final model for any given group of problems. From equation 9 it is evident that all the interior resistance elements along any given value of p' (fig. 59) must be alike to attain greatest simplicity in the model for the form of flow equation adopted. This condition has already been assumed in the development of equation 11. Thus, in any one

particular model, all values of $R_{\xi'}$ are the same except along the water table and confining bed, where they are twice the internal-element resistance ($2R_{\xi'}$), as previously discussed. $R_{\xi'}$ will be used henceforth to identify the resistance of the internal elements along p' lines and as a reference for calculating $R_{z'}$ by equation 12.

The interval $\Delta\xi$ defines the degree of subdivision along the ξ axis, and its selection partly determines the accuracy of the model results. Several calculated trial designs showed that $\Delta\xi=0.25$ would be satisfactory for providing adequate detail along the ξ axis.

Equations 9 and 12 and consideration of the difference between r_w and a sufficiently large r_e ordinarily found under field test conditions indicate that values of $R_{z'}$ must range over many orders of magnitude. Low-cost resistors can be obtained with values ranging from about 2×10^7 to about 2×10^{-1} ohms from commercial sources, and values of $R_{z'}$ were restricted to this range for economy of model construction. The test to be analyzed later was conducted on a well with a screen radius, r_w, of about 1 foot, in an aquifer about 100 feet thick. The value of Δz arbitrarily selected for the model is $m/20$; that is, the saturated thickness is divided by the chosen model grid into 20 equal increments along the z axis. At the well screen for such test-site dimensions and proposed model configuration, $\frac{\Delta z}{r\Delta\xi}=\frac{5}{1\times0.25}=20$. By referring to equation 12 and assuming an isotropic aquifer, it is seen that the ratio P_r/P_z equals unity and along the ordinate r_w represents the face of the well screen $(R_{z'})_{r_w}=400R_{\xi'}$, approximately. Unless the volume of the aquifer directly beneath the partially penetrating well is to be modeled, this latter relation provides an estimate of the largest value of $R_{z'}$ required in the model for the test case to be studied herein. From the limits of the resistor values economically available, the maximum value allowable for $R_{\xi'}$ would be about $R_{\xi'}=\frac{(R_{z'})_{r_w}}{400}=\frac{2\times10^7}{400}=5\times10^4$. A value of $R_{\xi'}$ less than the maximum is desirable to allow space in the vicinity of r_w in the model for control at smaller r values and treatment of anisotropic conditions. Thus a value $R_{\xi'}=1.8\times10^4$ ohms was finally, and only somewhat arbitrarily, selected. The distribution of resistance elements, $R_{z'}$ and $R_{\xi'}$, connecting all points (p', n') according to the reference system indicated on figure 62 is summarized in table 1.

The $R_{z'}$ values are given in table 1 as a function of $(P_r/P_z)(r/m)$ to present the model-design data in as general a form as possible. A model constructed according to table 1 may be used for analyzing any pumping test in which the values of r/m lie within the range given

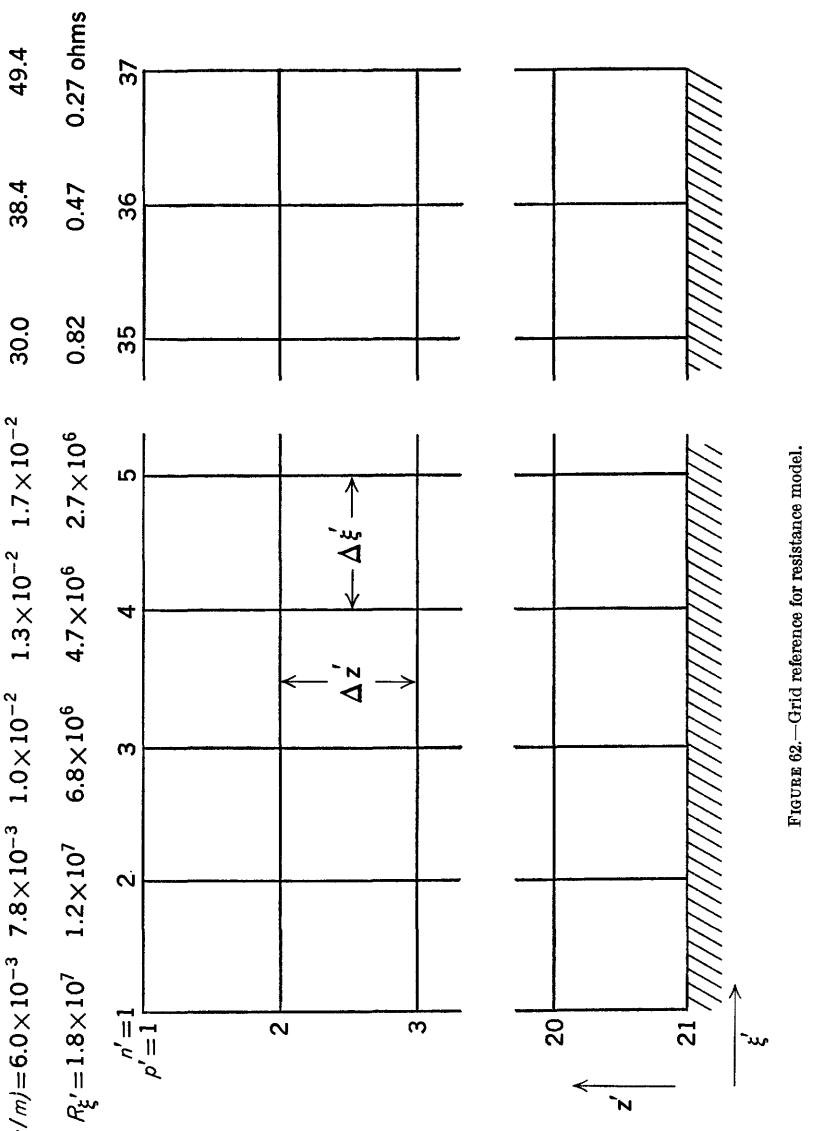

FIGURE 62.—Grid reference for resistance model.

there because of the dimensional characteristics of equation 12. For example, $n'=3$, where $(P_r/P_z)(r/m)=1.00\times10^{-2}$ could be used to model a pumping well with a radius $r_w=0.1$ foot in an isotropic aquifer 10 feet thick, or a well with a radius of 10 feet in an isotropic aquifer 1,000 feet thick, or any other combination of r_w and m for which $(P_r/P_z)\ (r/m)=1.00\times10^{-2}$.

According to equation 10, $(r_n/m)/(r_{n-1}/m)=e^{\Delta\xi}$. The latter relation was used for calculating succeeding values of $\left(\frac{P_r}{P_z}\right)\left(\frac{r}{m}\right)$, as given in table 1, by assuming that $\Delta\xi=0.25$ and by beginning the grid computations arbitrarily at a value of $\left(\frac{P_r}{P_z}\right)\left(\frac{r}{m}\right)=5\times10^{-4}$. With the successive values of $\left(\frac{P_r}{P_z}\right)\left(\frac{r}{m}\right)$ calculated in this way and the other model-design assumptions that $\Delta z=0.05m$, $R_{\xi'}=1.8\times10^4$ ohms, equation 12 was used to calculate $R_{z'}$ for each value of n'. Because values of r/m for nonspecific test sites will seldom be predictable integers, the actual numerical value of r/m selected at any particular intersection along ξ is immaterial, if the resistor grid is to be used for more than one test analysis. In most cases each pumping-test analysis will require a model solution for P_z by equation 14 for several assumed values of r_w/m. The P_z values computed in this way may then be used for interpolation to find the exact value of P_z for the observed r_w/m at the test site. This appears to be a more economical procedure than constructing a completely new model or resistor grid for each test analysis.

TABLE 1.—*Summary of* $R_{z'}$ *values for* $R\xi'=1.8\times10^4$ *ohms,* $\Delta z=0.05$m, *and* $\Delta_\xi=0.25$ *(fig. 62)*

n'	$\frac{P_r}{P_z}\frac{r}{m}$	Calculated $R_{z'}$ (eq 12)	$R_{z'}$ nominal resistance in ohms (±10 percent)	n'	$\frac{P_r}{P_z}\frac{r}{m}$	Calculated $R_{z'}$ (eq 12)	$R_{z'}$ nominal resistance in ohms (±10 percent)
1	6.03×10^{-3}	1.94×10^{7}	1.8×10^{7}	20	7.04	1.45	1.5
2	7.82	1.18	1.2	21	9.04×10^{-1}	8.80×10^{2}	8.2×10^{2}
3	1.00×10^{-2}	7.14×10^{6}	6.8×10^{6}	22	1.16×10^{0}	5.34	5.6
4	1.29	4.33	4.7	23	1.49	3.24	3.3
5	1.66	2.62	2.7	24	1.91	1.96	1.8
6	2.13	1.59	1.5	25	2.46	1.19	1.2
7	2.73	9.67×10^{5}	1.0	26	3.16	7.22×10^{1}	6.8×10^{1}
8	3.50	5.86	5.6×10^{6}	27	4.05	4.38	4.7
9	4.50	3.56	3.3	28	5.20	2.66	2.7
10	5.78	2.15	2.2	29	6.68	1.61	1.5
11	7.42	1.31	1.2	30	8.58	9.78×10^{0}	1.0
12	9.53	7.92×10^{4}	8.2×10^{4}	31	1.10×10^{1}	5.94	5.6×10^{0}
13	1.22×10^{-1}	4.82	4.7	32	1.41	3.60	3.9
14	1.57	2.92	2.7	33	1.81	2.18	2.2
15	2.02	1.77	1.8	34	2.33	1.32	1.2
16	2.59	1.07	1.0	35	3.00	8.03×10^{-1}	8.2×10^{-1}
17	3.32	6.51×10^{3}	6.8×10^{3}	36	3.84	4.88	4.7
18	4.27	3.95	3.9	37	4.94	2.95	2.7
19	5.48	2.39	2.2				

ANALOG STUDY OF PUMPING-TEST DATA

ANALYSIS OF GRAND ISLAND PUMPING TEST

The resistance analog shown on figure 62 was used to study pumping-test data collected near Grand Island, Nebr., and was reported by Wenzel (1942, p. 117–122). At the test site, the aquifer is about 100 feet thick and is composed of unsorted sand and gravel. Permeability coefficients determined by laboratory tests on disturbed samples are shown in table 2. The well pumped in the test was 24 inches in diameter and extended about 37.1 feet below the static water table. It was pumped continuously at a rate of about 540 gpm for 48 hours. During the period of pumping, drawdowns were observed in 80 nearby wells that were located at distances that ranged from 2.6 feet to 1,217.1 feet from the pumped well.

Although it is evident from table 2 that the aquifer in profile is not homogeneous, it will first be assumed homogeneous and isotropic. Thus, $P_r/P_z=1$. (Other situations are discussed on p. 231–234.) In the resistor grid shown on figure 62, $\Delta\xi=0.25$, $\Delta z=m/20=5$ feet, and $R_{\xi'}=1.8\times10^4$ ohms. Therefore, from equation 12, the value of $R_{z'}$, corresponding with the position of r_w is

$$R_{z'}=\left(\frac{\Delta z}{r_w\Delta\xi}\right)^2 R_{\xi'}=\left(\frac{5}{1\times0.25}\right)^2\times1.8\times10^4=7.2\times10^6 \text{ ohms.}$$

From table 1, it is seen that the radius r_w is very nearly represented by $n'=3$ on the resistance analog design given.

The drawdown in the pumped well was about 20 feet during the last part of the test period (Wenzel, 1942, p. 150). It was probably somewhat smaller during the first few minutes of pumping; and as indicated by Wenzel (1942, p. 150), the drawdown of the water table outside the well face was much less. But for illustration here, 20 feet is assumed to be a satisfactory approximation of the drawdown in the pumped well. Because the pumped well was perforated along its full length (Wenzel, 1936, p. 28), the effective drawdown at any point along the well bore, but above the pumping level, numerically equals the depth of that point below the initial static water level. At all points below the pumping level in the pumped well, the head decline is very nearly 20 feet, assuming that flow between the screen and pump intake occurs with negligible head loss within the well. These relations are shown, in terms of s/s_w, on figure 63 at the corresponding model grid intersections. The analogic electric controls established on the model for the first few minutes of pumping ($t=0+$) must reproduce the same head distribution as shown in figure 63. It has already been stated that voltage in the analog is proportional

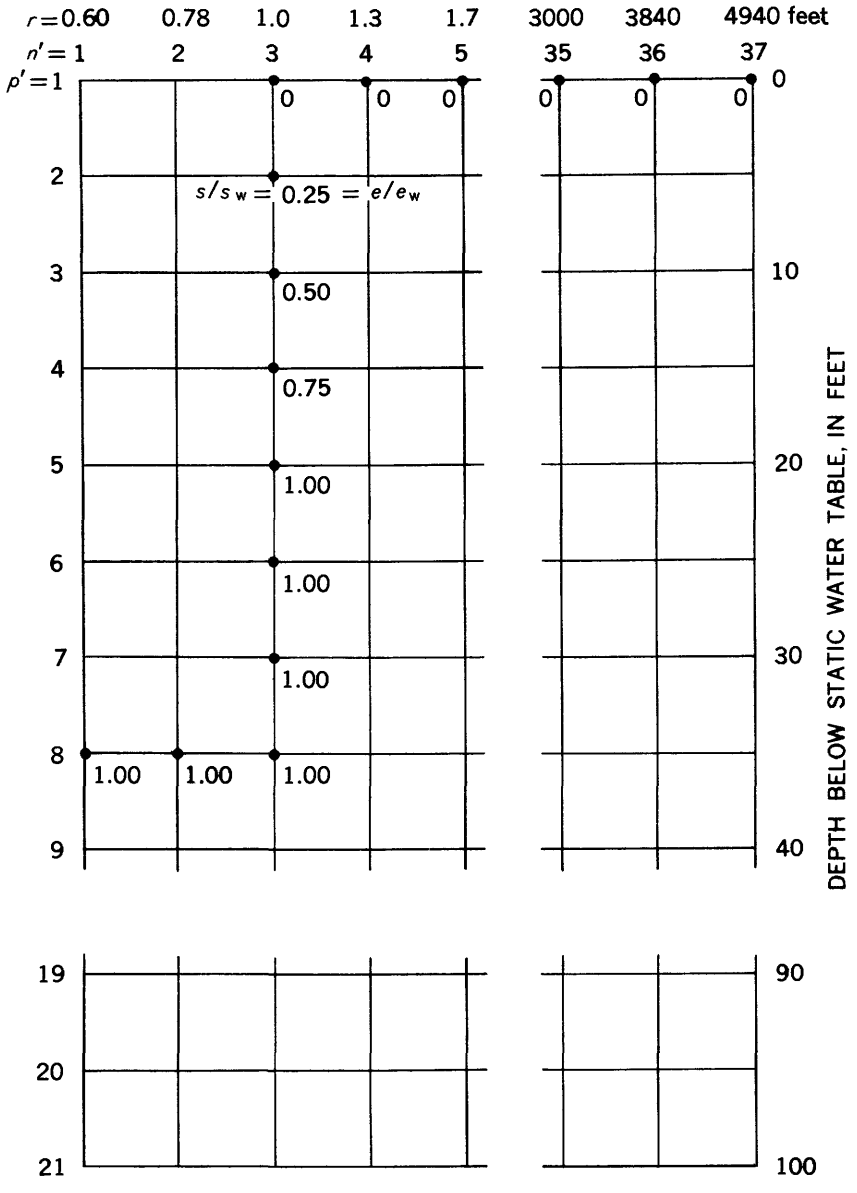

FIGURE 63.—Drawdown conditions at t=0+ for Grand Island pumping test in relation to model grid intersections.

to drawdown in the aquifer. Therefore at all control points along the boundary the relation between voltage and drawdown may be expressed as

$$\frac{s_{(p,n)}}{s_w} = \frac{e_{(p',n')}}{e_w}, \tag{15}$$

where e_w refers to the maximum voltage applied on the analog-boundary points corresponding with points similarly located along the well screen.

TABLE 2.—*Laboratory determinations of permeability of samples of alluvium from well 84, Grand Island, Nebr.*

[After Wenzel, 1942, p. 118]

Depth below water table (ft)	P (gpd per sq ft)	Depth below water table (ft)	P (gpd per sq ft)
0–2. 4	480	43. 4–47. 4	780
2. 4–8. 4	1, 685	47. 4–53. 4	730
8. 4–12. 4	1, 460	53. 4–58. 4	2, 095
12. 4–17. 4	1, 095	58. 4–63. 4	1, 050
17. 4–22. 4	1, 095	63. 4–70. 4	2, 185
22. 4–31. 4	4, 350	70. 4–78. 4	220
31. 4–32. 4	2	78. 4–84. 4	495
32. 4–34. 4	925	84. 4–91. 4	430
34. 4–38. 4	150	91. 4–97. 4	285
38. 4–43. 4	350		

To find the relative drawdowns occurring during the first few minutes of pumping, voltage was controlled at grid intersections (nodes) in accordance with figures 63 and equation 15. Readings were then made of the voltage at each node. The relative drawdown contours developed from these measurements are shown in figure 64. Instrumental limitations precluded definition of the drawdown configuration at the larger radii, but the contribution to flow from that region was found to be insignificant during the first few minutes of pumping and may be neglected. Values of s/s_w observed along $p'=2$ on the model were used in obtaining the curve shown on figure 65, which is a graph of r versus $r(\Delta s/s_w)$ per Δz. Note that because $s/s_w=0$ at all $p'=1$, the observed s/s_w along $p'=2$ equals the difference between drawdown ratios through a depth Δz. Because these measurements are made near the water-table position, they closely reflect the gradient found just beneath the water table. The latter curve is a convenient form for obtaining P_z from a finite-difference form of equation 14. In the relation

$$\frac{Q\Delta z}{P_z s_w}=-2\pi \sum_{r_w}^{r_e} r(\Delta s/s_w)_{\Delta z1}\Delta r, \tag{16}$$

in which $(\Delta s/s_w)_{\Delta z1}$ refers to the gradient observed just beneath the analog water-table position, between $p'=1$ and $p'=2$ (fig. 62). The summation in equation 16 is equivalent to the integral of equation 14, wherein constants have been removed from under the summation upon expression in terms of finite differences. The summation of

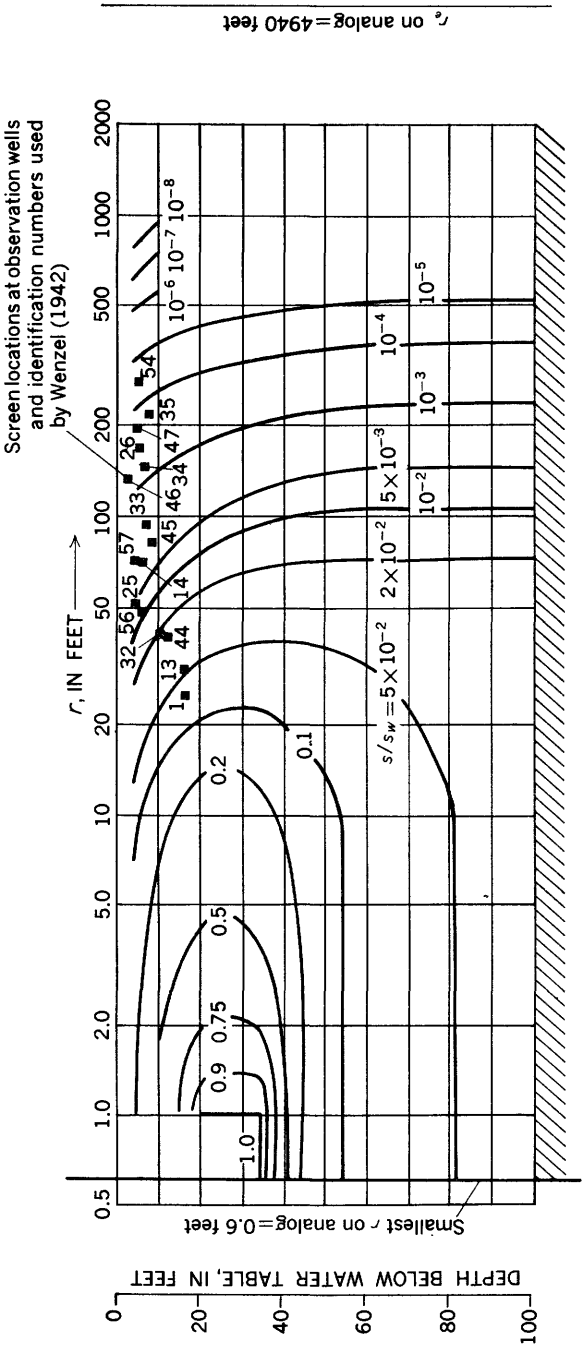

FIGURE 64.—Initial drawdown configuration ($t=0+$) in terms of s/s_w assuming partial penetration and isotropy, Grand Island pumping-test site, Nebraska.

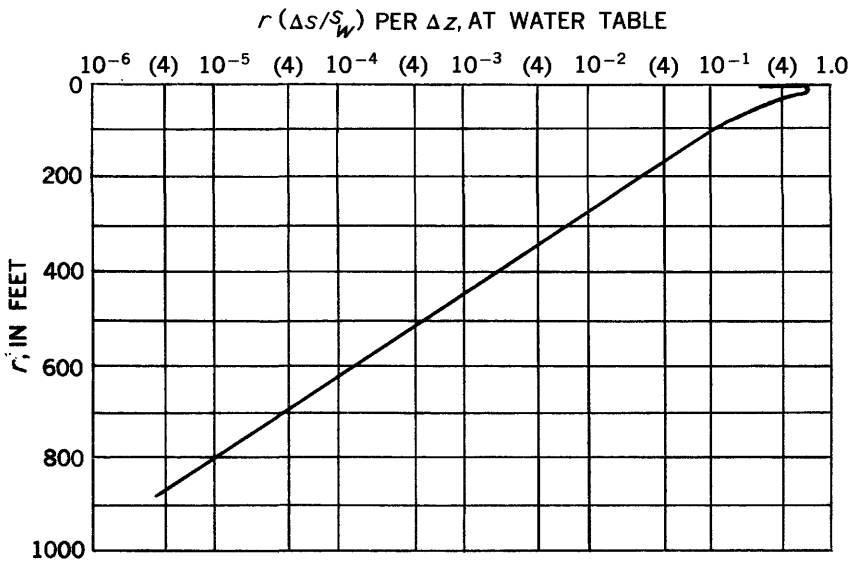

FIGURE 65.—Initial vertical gradients along the water table and their relation to radius from the pumped well, Grand Island pumping-test site.

equation 16 was evaluated for the study reported in figure 64 by graphically summing the area under the curve of figure 65 from which

$$\sum_{r_w=1}^{r_e=660} r(\Delta s/s_w)_{\Delta z1}\Delta r = -57.7$$

and

$$P_\xi = P_z = \frac{540\times 1{,}440\times 5}{20\times 2\pi\times 57.7} = 536 \text{ gpd/ft}^2 \text{ (for } s_w = 20 \text{ ft)}$$

or

$$= 1{,}072 \text{ gpd/ft}^2 \text{ (for } s_w = 10 \text{ ft}).$$

The numerical result for $s_w=20$ feet is not in particularly close agreement with Wenzel's $P=1{,}000$ gpd per sq ft obtained from analysis of later parts of the pumping-test data by other methods. The average permeability to horizontal flow should be about 1,200 gpd per sq ft, according to table 2. An assumed value of 10 feet for the drawdown in the pumped well may therefore be more nearly correct than the 20 feet assumed from the test for the model analysis of the flow occurring during the first few minutes of pumping.

However, other features of the Grand Island test and test site depart more fundamentally from the assumptions used in the model analysis. Study of these features is pursued in the following discussion not so much to obtain good numerical agreement between the model analysis and the more conventional forms of aquifer-test analyses as to illustrate those features of flow to wells that are signifi-

cantly related to the effects of vertical flow components, nonhomogeneity, and anisotropy.

Several interesting problems are associated with the computation of specific yield using equation 13 for the Grand Island test area. In obtaining the solution presented on figure 64, it was assumed that the drawdown along the water table was zero. The length of the time interval over which this condition is approximately satisfied in the field is critical for several reasons. Chiefly, it is important because it identifies the time interval over which the slopes of hydrographs for observation wells represent only the initial rate of downward movement of the water table. Boulton (1954, p. 572) has indicated that the flow pattern varies only slightly from its initial form in the interval $0<\frac{Pt}{S_y m}<0.05$. Thus the test-time interval for valid analysis by equations 13 and 14 is from $t=0$ to $t=0.05\ S_y m/P$, approximately. By use of Wenzel's results for S_y and P for the Grand Island test, it is seen that the critical time interval is evidently from $t=0$ to $t=0.05\times0.2\times100\times7.48/1{,}000=7.48\times10^{-3}$ day, or about 11 minutes. Hence, the hydrograph slopes observed in the field during about the first 10 minutes of pumping should adequately represent the flow regime resulting from the model boundary conditions assumed in developing figure 64, provided that the specific yield during the interval was approximately 0.2.

Fully defined hydrographs for the first few minutes of the Grand Island test cannot be constructed, because water-level measurements in the observation wells were made rather infrequently. A selected group of wells with the data used herein for computing S_y are listed in table 3 in order of distance from the pumped well. The selection from Wenzel's data and the listing of wells was made on the basis that (1) the wells were measured to determine drawdown at least once during the first 10 minutes of pumping, (2) the well depth and diameter are known, (3) a measurable drawdown occurred in the well during the first 10 minutes of pumping, and (4) the well ends in the upper part of the zone of saturation. Selected hydrographs are given on figure 66. The distance of each listed well from the pumped well and the depth below the water table at which each is finished are shown on figure 64.

Factors related to data collection and test operation that might invalidate the estimate of S_y, using equation 13, will be discussed later. At this point it is of interest to proceed directly to the solution for S_y along the analytical lines already defined. Toward this end,

an estimated value of $\partial s/\partial t$ was obtained for each of the wells listed in table 3 by dividing the observed drawdown noted in the first measurement made by the time elapsed since pumping began. The time

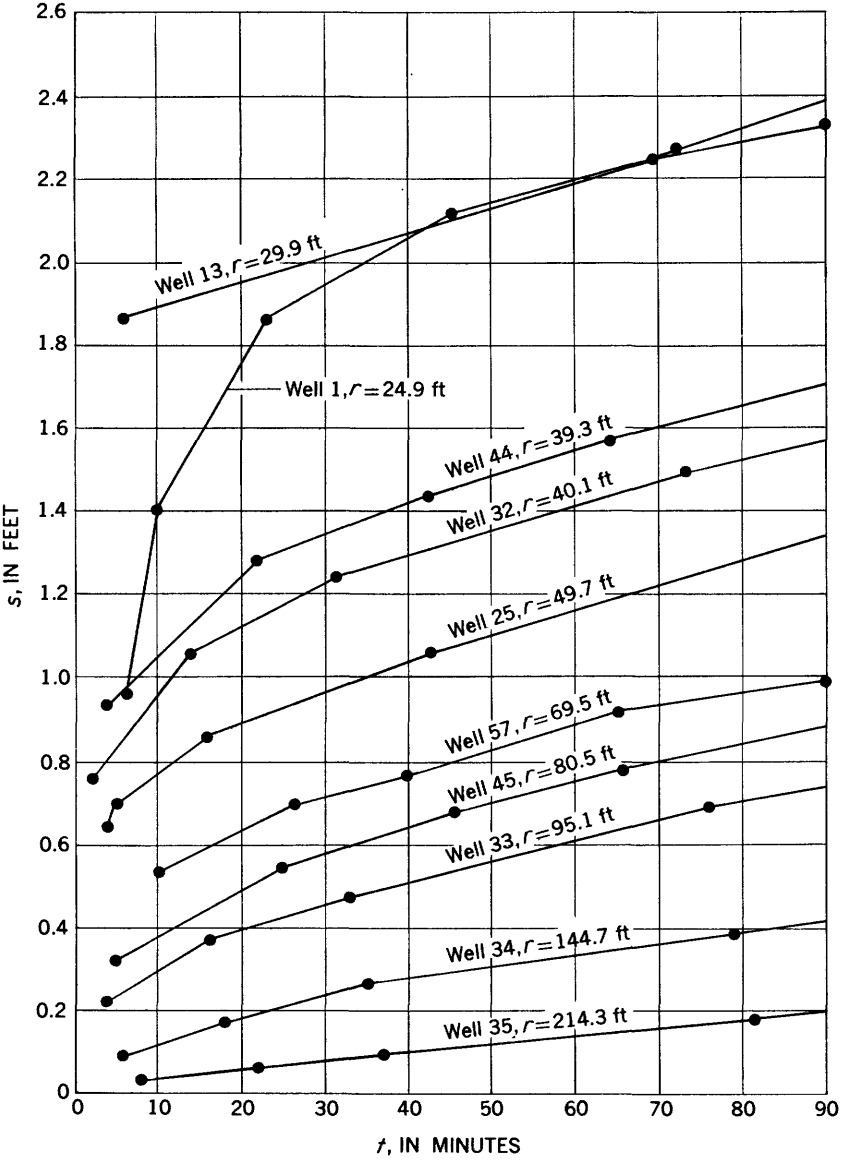

FIGURE 66.—Hydrographs of selected observation wells, Grand Island pumping-test site.

TABLE 3.—*Water-level data from selected wells and specific yield calculated from model solution*

Data from Wenzel (1942, p. 120, 151-171)					Values obtained from model study	
Well	r (ft)	Δt_1 time first drawdown measured (minutes)	$(\Delta s)_{t1}$ for first time interval (ft)	$\frac{\partial s}{\partial t} \simeq \frac{(\Delta s)_{t1}}{\Delta t_1}$ $\left(\frac{\text{ft}}{\text{day}}\right)$	$\frac{\partial s}{\partial z} \simeq \frac{(\Delta s)_{\Delta z1}}{\Delta z}$ (nondimensional)	$S_y = \frac{536}{7.48} \frac{\Delta s_{\Delta z1}/\Delta z}{(\Delta s)_{t1}/\Delta t_1}$ $= 71.7 \frac{\Delta s_{\Delta z1}/\Delta z}{(\Delta s)_{t1}/\Delta t_1}$ (nondimensional)
1	24.9	6	0.96	230	9.6×10^{-2}	2.98×10^{-2}
13	29.9	6	1.87	448	7.0	1.13×10^{-2}
44	39.3	4	.93	335	4.15	8.87×10^{-3}
32	40.1	2	.75	540	3.9	5.17×10^{-3}
56	46.7	7	.88	181	2.8	1.11×10^{-2}
25	49.7	4	.64	231	2.4	7.45×10^{-3}
57	69.5	10	.53	76.3	1.14	1.07×10^{-2}
14	70.0	9	.49	78.3	1.14	1.04×10^{-2}
45	80.5	5	.32	92.2	8×10^{-3}	6.22×10^{-3}
33	95.1	4	.22	79.2	5.3	4.8×10^{-3}
46	130.3	7	.10	20.6	2.36	8.2×10^{-3}
34	144.7	6	.09	21.6	1.88	6.23×10^{-3}
26	170	7	.05	10.3	1.07	7.43×10^{-3}
47	195.6	9	.05	8.0	6.6×10^{-4}	5.37×10^{-3}
35	214.3	8	.03	5.4	4.67	6.2×10^{-3}
27	270	9	.01	1.5	1.82	8.7×10^{-3}

interval between commencement of pumping and the first drawdown measurement, Δt_1, and the corresponding drawdown $(\Delta s)_{t1}$ are given in table 3. Estimates of $\frac{\partial s}{\partial z}$ were obtained directly from the model study as

$$\frac{\partial s}{\partial z} \simeq \frac{(\Delta s)_{\Delta z1}}{\Delta z} = s_w(e_{p'=2} - e_{p'=1})/e_w \Delta z = 4e_{p'=2}/e_w,$$

for $s_w = 20$ feet, $e_{p'=1} = 0$, and $\Delta z = 5$ feet. Given in the last column of table 3 are values of S_y calculated from the relation

$$S_y = P_z \frac{(\Delta s)_{\Delta z1}/\Delta z}{(\Delta s)_{t1}/\Delta t_1}, \tag{17}$$

which is a finite-difference approximation of equation 13. The value of P_z used was $536/7.48 = 71.7$ feet per day as obtained from equation 16 and graphical analysis of figure 9.

The values of S_y, calculated from data collected during the first few minutes of pumping arrayed in table 3, are in disagreement with the value of 0.2 determined by Wenzel from the more commonly employed mathematical equations. In general, the results from the model study are, at least, an order of magnitude smaller than those obtained by Wenzel (1942, p. 125). Thus far, however, treatment of the test data has been rather superficial in that gross assumptions have been made regarding their meaning, and the aquifer itself has been modeled somewhat arbitrarily. Further investigation of the effects of these idealizing assumptions on the calculated results is

warranted. A summary of the numerical results obtained from the model study to this point suggests that calculated permeability is very nearly equal to, or is about one-half the value found by Wenzel (P=1,000 gpd per sq ft), depending on the applicable value of s_w. Specific yield calculated from the model study is about one order of magnitude smaller than that calculated by Wenzel.

These results indicate that possibly the values of $(\Delta s)_{\Delta z1}/\Delta z$ obtained from the model analysis are too small or that the assumptions attending data interpretation have resulted in values of $(\Delta s)_{t1}/\Delta t$ that are too large. The present model configuration is not entirely a realistic analog of the Grand Island aquifer, and the hydrograph slopes appear to have been crudely estimated. Therefore, attention is focused on investigation of the validity of the model and the data used in obtaining values of the ratio $(\Delta s)_{t1}/\Delta t_1$.

ANALOGIC RELATIONS

The resistance analog used for obtaining the drawdown distribution in the aquifer was constructed by assuming that the effects of internal storage on flow are negligible. This was stated as $S'\frac{\partial s}{\partial t}=0$ in developing equation 5 from equation 3. If internal storage changes are significant, they tend to dampen the response of the water-table fluctuations. Thus the computed values of $(\Delta s)_{t1}/\Delta t_1$ would be relatively small and values of S_y calculated from the model analysis would be larger than the values calculated from the more commonly used mathematical relations. A very approximate appraisal of this effect might be made by comparing the volume pumped during the first few minutes of the test with the total change in water stored between the water table and the confining bed underlying the aquifer as a result of lowered heads in that region. The total change in volume of water stored beneath the water table may be expressed in finite-difference form as

$$\Delta V=2\pi S'm\sum_{r_w}^{r_e} r\Delta r(\Delta s)_m, \tag{18}$$

where $(\Delta s)_m$ is the average drawdown along the z axis at radius r. The coefficient of bulk compressibility of water is about 5×10^{-5} per atmosphere, or about 1.5×10^{-6} per foot of water (Dorsey, 1940, p. 245). According to Birch (1942, p. 61) the coefficient of bulk compressibility of the common rock types is about 4×10^{-6} per atmosphere, or about 1.3×10^{-7} per foot of water. Thus, for an assumed aquifer porosity of 0.3, the internal unit storage coefficient is (very) approximately $S'=1.5\times0.3\times10^{-6}+1.3\times0.7\times10^{-7}=5.4\times10^{-7}$. The summation in equation 18 for the data of figure 64 and s_w=20 feet was found

by graphical analysis to equal 3,800. Substituting this sum, as well as appropriate values for the other terms in equation 18, yields

$$\Delta V = 2\pi \times 5.4 \times 10^{-7} \times 1 \times 10^{2} \times 3.8 \times 10^{3} = 1.3 \text{ cubic feet.}$$

Evidently, for the conditions postulated in the flow field, the initial drawdown distribution could be formed with little change in internal storage. The source of greatest error in the above estimate is probably the figure for S'. However, an error of two orders of magnitude in S' would at most account for a volume of water pumped from the aquifer during only the first 2 minutes. The value of S' used here probably is not in error by this much. The effect of internal storage release on changes in the water-table position is, therefore, believed to be virtually negligible during the first 10 minutes of pumping.

Aside from consideration of the volumetric changes below the water table, the values of S_y summarized in table 3 also lend support to this belief. If release from internal storage were damping water-level changes appreciably, the calculated values of S_y should show an increase with increasing r. This is because $(\Delta s)_{t1}/\Delta t_1$ would become progressively smaller than for the case of zero internal storage for increasing r. Data in table 3 indicate no such trend in the relation between S_y and r.

Use of equation 17 for calculating S_y presumes that $(\partial s/\partial r)^2$ is very small compared with $\partial s/\partial z$ and that $\partial s/\partial z$ is small for the time interval used in analysis. These are the conditions at the water table prerequisite to pass from the conditions of equation 4 to those of equation 13 for an isotropic aquifer. The Grand Island data may be used directly as an independent check on the validity of these approximations. Both $\partial s/\partial t$ and $\partial s/\partial r$ may be estimated from the test data by finite-difference or graphical methods. Use of Wenzel's values of S_y and P (0.2 and 1,000 gpd per sq ft, respectively) in a finite-difference form of equation 4, assuming $P_r = P_z$, permits a solution for $\partial s/\partial z$. A comparison between the computed value of $\partial s/\partial z$ and $\frac{S_y}{P}\frac{\partial s}{\partial t}$ will indicate the importance of the radial-flow component at the water table. According to Boulton's criteria for testing the validity of these approximations, time is the only significant variable. Thus it will suffice to perform the indicated check at only one value of r. A radius of 50 feet was selected arbitrarily and calculations were made for times of 30, 300, and 2,000 minutes after pumping began. An example of the data plots used is given on figure 67. Using the finite-difference approximations developed

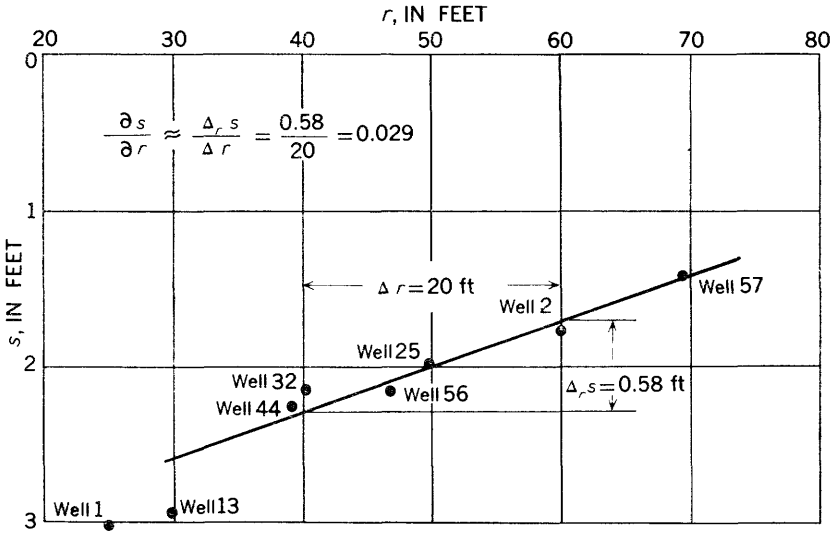

A. Drawdown profile for $t=300$ minutes

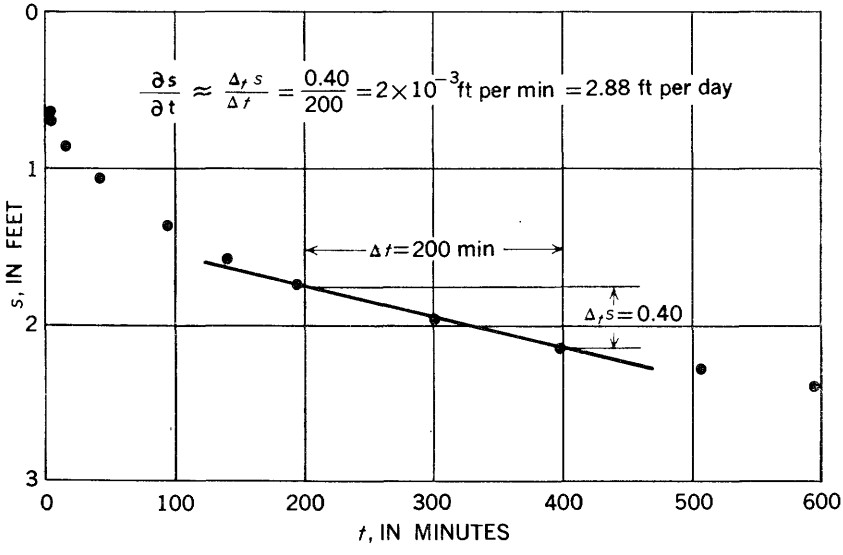

B. Drawdown in well 25

FIGURE 67.—Drawdown data used for estimating $\partial s/\partial r$ and $\partial s/\partial t$ at $r=50$ feet, $t=300$ minutes. *A*, Drawdown profile for $t=300$ minutes; *B*, Drawdown in well 25.

on figure 67, taking $S_y/P=0.2/140$ (from Wenzel), and letting $(\partial s/\partial z)=a$ in equation 4 yield

$$\frac{0.2}{140}\times 2.88=(0.029)^2+a^2-a$$

$$4.12\times 10^{-3}-8.4\times 10^{-4}=3.28\times 10^{-3}=a^2-a,$$

from which $a=-3.27\times 10^{-3}$ or $+1.00327$. For the boundary conditions considered here $(\partial s/\partial z)>0$ is impossible, and the real solution is given by $a=-3.27\times 10^{-3}$. A similar computation, using

$$\frac{S_y}{P}=\frac{7.48\times 1\times 10^{-2}}{5.36\times 10^2}=1.4\times 10^{-4}\text{ day/ft},$$

from the model study results in the following:

$$2.88\times 1.4\times 10^{-4}=(0.029)^2+a^2-a$$

$$4.0\times 10^{-4}-8.4\times 10^{-4}=-4.4\times 10^{-4}=a^2-a,$$

from which $a=+4.4\times 10^{-4}$ or $+0.9996$, approximately. Neither of these values can be reconciled with the known features of the flow field. Thus it is apparent that the $\frac{S_y}{P}$ ratio developed from model analysis of the data collected during the first few minutes of pumping is probably incorrect, at least for $t=300$ minutes. S_y may have been considerably larger than 0.01 at $t=300$ minutes.

Using Wenzel's values for S_y and P, estimates of $\partial s/\partial z$ were also made for $r=50$ feet, $t=30$ minutes, and $t=2{,}000$ minutes. The data employed and computed results are given in table 4. At those times for which the numerical values of $-a$ are nearly equal to $(S_y/P)\,\Delta_t s/\Delta t$, the water-table fluctuations are predominantly influenced by vertical-flow components. This can be recognized directly from the physical implications inherent in equation 4. To provide some numerical description of the relative effects of vertical or horizontal gradients on the rate of change of the water-table position, we may use, for example, the ratio $(a^2-a)/(S_y\Delta_t s)/P\Delta t$. From table 4, for $t=30$ minutes, this ratio equals 0.967, which means that 96.7 percent of the rate of change of the water-table position was caused by the vertical component of gradient beneath the water table at $t=30$ minutes. Or, using the complementary ratio, $(\partial s/\partial r)^2/(S_y\Delta_t s)/P\Delta t$, one finds that only 3.3 percent of the rate of change of the water-table position was caused by the radial component of gradient beneath the water table. As time increases, the radial components of gradient become increasingly more significant. For the data of table 4, the vertical

component of gradient accounts for 79.4 percent at $t=300$ minutes and 14.6 percent at 2,000 minutes of the rate of change of the water-table position. Thus, even after 30 minutes of pumping, equations 13 and 17 may be satisfactory approximations of equation 4 for some purposes, because radial components appear to have a comparatively small effect on $\frac{\partial s}{\partial t}$ at the water table. However, these comparisons are highly dependent on the value of S_y and P. If it is assumed that $S_y/P=1.4\times10^{-4}$, obtained from analysis of data summarized on figures 64 and 65, the rate of change of the water-table position appears to be controlled equally by radial- and vertical-flow components after pumping for 30 minutes. Information on the value of S_y developed from the model analysis is inconclusive. Nevertheless, it seems reasonable to conclude that the vertical-flow components were predominant in regulating the movement of the water table during at least the first 10 minutes of pumping, if one restricts his analysis to the use of S_y values indicated by the model study. Evidently, for data collected during the early part of the Grand Island test, analytical methods based on the assumption that vertical-flow components are everywhere negligible yield spurious results at all times.

TABLE 4.—*Estimates of* $\frac{\partial s}{\partial z}$ *at the water table from drawdown data* ($r=50$ *ft*)

[All calculations based on S_y and P from Wenzel (1942, p. 122–127)]

t (minutes)	Observed $\frac{\Delta_t s}{\Delta t}$ (feet per day)	Observed $-\frac{\Delta_r s}{\Delta r}$	Estimated $-\frac{\partial s}{\partial z}$	Observed $\frac{S_y \Delta_t s}{P \Delta t}$
30	10.7	2.7×10^{-2}	1.44×10^{-2}	1.53×10^{-2}
300	2.88	2.9×10^{-2}	3.27×10^{-3}	4.12×10^{-3}
2,000	.452	2.35×10^{-2}	9.4×10^{-5}	6.46×10^{-4}

AQUIFER REPRESENTATION

Among the foregoing analyses, it has been assumed that the aquifer is homogeneous and isotropic and is effectively 100 feet thick, and the analytical results have been reviewed somewhat with the notion that S_y is independently constant in both time and space. Equation 4, or an appropriate form derived from equation 4, might be utilized directly in conjunction with detailed field measurements of $\Delta_r s/\Delta r, \Delta_z s/\Delta z$, and $\Delta_t s/\Delta t$ for calculating S_y as a function of time. The drawdown configuration from the Grand Island test observations is inadequate for this purpose. Thus a satisfactory estimate of S_y appears to be impossible to obtain from equation 4. Rather, one must rely on the model study for permeability and on a compara-

tively indirect estimate of S_y by utilizing observed values of $(\Delta s)_{t1}/\Delta t_1$, as in the development shown in table 3. But here one finds gross uncertainties.

Obviously, from table 2, the aquifer is stratified to some degree. (See also table *in* Wenzel, 1942, p. 118). The assumed thickness of 100 feet, heretofore accepted, may be effectively much less. Note the section of comparatively low permeability listed between depths of 31.4 and 32.4 feet below the water table. If this section is representative of an extensive lense, the pumped well might be considered as fully penetrating an aquifer 31.4 feet thick. Such a model representation may be more correct for the first few minutes of pumping than the one adopted in developing figure 64. Values of s/s_w in the profile, obtained from a model by assuming that the pumped well fully penetrates an aquifer 31.4 feet thick and that the aquifer is isotropic, are shown on figure 68. The data of figure 68, graphically

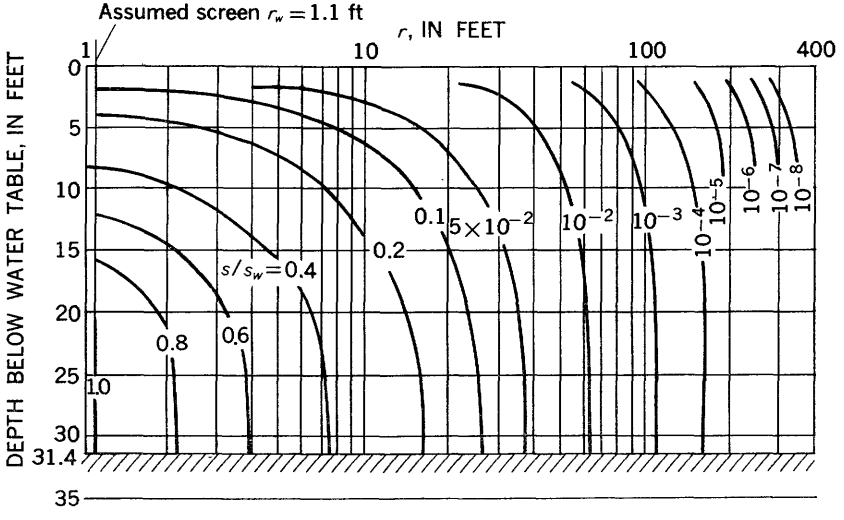

FIGURE 68.—Initial drawdown configuration ($t=0+$) in terms of s/s_w, assuming full penetration to depth of 31.4 feet, and $P_r = P_s$.

analyzed by means of equation 16, yield a permeability of about 630 gpd per sq ft, if one assumes that $s_w=20$ feet. The permeability calculated from the model, if one assumes a partial penetration of the aquifer 100 feet thick, was about 540 gpd per sq ft. A solution for S_y by use of equation 17, which uses data from Wenzel's well 35 at $r=214$ feet and the model study of full penetration of an aquifer 31.4 feet thick, yields $S_y=1\times10^{-4}$. From table 3, the corresponding analysis for partial penetration of the aquifer 100 feet thick gave

$S_y=6.2\times10^{-3}$. Thus the assumption of $m=31.4$ feet yields a permeability coefficient more nearly in agreement, and S_y value in poorer agreement, with Wenzel's results than the modeling assumption of $m=100$ feet.

Unconsolidated rocks are almost invariably stratified to some extent, generally along nearly horizontal bedding planes. This produces a preferentially high horizontal permeability and a comparatively low vertical permeability. Data in table 2 indicate that the aquifer is not homogeneous vertically, or in the direction of the z axis. If the entire aquifer thickness is considered, the gross permeability to one-dimensional flow along the z axis is only slightly more than 2 gpd per sq ft, and to one-dimensional horizontal flow, the gross aquifer permeability is about 1,200 gpd per sq ft. Thus results obtained from the model design employed are probably in considerable error, and this error can be reduced adequately only by accounting for nonhomogeneities in the selection of $R_{z'}$ values in the resistance network. Unless appropriately taken into account, anisotropy due to horizontal bedding of fine materials will also contribute to errors in calculated values of permeability and specific yield.

As an example, full penetration to a depth of 31.4 feet was also studied by assuming homogeneous anisotropy with $P_r/P_z=26$. On the model, the well-screen radius is represented for this ratio of P_r/P_z at $n'=1$, as can be found by comparing the computed value of $R_{z'}$ from equation 12 with the model-resistance data on table 1. From the model study and test data: $P_r=1{,}300$ gpd per sq ft, $P_{z'}=49$ gpd per sq ft, and $S_y=2.8\times10^{-3}$ (from the data of well 35).

Drawdown data might be collected in the field specifically for finding the ratio P_r/P_z directly. Drawdowns could be measured in wells screened at an array of appropriate grid intersections, indicated schematically by closed circles on figure 58. Observations made simultaneously at an array of wells positioned as shown—with $\Delta\xi$, r_n, and Δz known—would provide a direct solution for P_r/P_z from equation 9. With the ratio P_r/P_z found independently, the model grid location for r_w is easily obtained directly through equation 12. In turn, this offers a sound approach to calculating P_z by model analysis through equation 16.

A summary of the analog test results obtained for this report is given in table 5. The numerical results are not significant hydrologically, but they do serve to emphasize the need for adequately defining the test site and analyzing the pumping-test data and model accordingly. Without such knowledge, pumping-test analysis is indeterminate if vertical-flow components are appreciable.

DEPTH, PENETRATION, AND TIMELAG OF OBSERVATION WELLS

In the preceding analysis of the Grand Island pumping test, data from observation wells were assumed to yield correct values of $(\Delta s)_{\Delta z1}/\Delta z$ and $(\Delta s)_{t1}/\Delta t_1$ without qualification. A comparison of the field conditions with the nature of the flow model reveals certain inconsistencies that affect the calculated permeability and specific yield. A review of these inconsistencies permits identification of improved field data-collection practices, designed to fit the electronic-model analysis of pumping-test information.

TABLE 5.—*Summary of values of permeability and specific yield calculated from model studies of Grand Island, Nebr. pumping-test data, well 35*

Assumptions	P_r	P_z	S_y
Well penetrates aquifer, 100 feet thick, to depth of 40 feet. Aquifer homogeneous and isotropic	540	540	6.2×10^{-3}
Well penetrates aquifer, 31.4 feet thick, to depth of 31.4 feet. Aquifer homogeneous and isotropic	630	630	1.0×10^{-4}
Well penetrates aquifer, 31.4 feet thick, to depth of 31.4 feet. Aquifer homogeneous and anisotropic	1,300	49	2.8×10^{-3}

Observation wells employed in the Grand Island test were either 3 inches or 1 inch in diameter. The 1-inch wells were fitted with 18-inch long screened drive points, and the 3-inch wells were open to the aquifer only through holes in jetting points attached to the lower end of the well casing (Wenzel, 1936, p. 29). The 3-inch wells probably had a smaller efficiency for admitting flow from the aquifer to the well bore, and they certainly had a higher storage capacity per unit depth than the 1-inch wells. Thus it is evident that the 3-inch wells would respond more slowly to a sudden change in pressure in the aquifer than the 1-inch wells. On figure 66, the hydrograph of well 25, a 3-inch well, may be compared with the hydrographs of wells 44, 32, 57, and 45, all 1-inch wells. For these data, differences in timelag from an applied pressure change are not noticeable for times of the order of 10 minutes or more. Differences in the hydraulic conditions found at individual observation-well screens or holes may account for a wide range in response characteristics. This may be the reason for the great differences between hydrographs of wells 1 and 13 during the first 40 minutes of pumping. Both are 3 inches in diameter and penetrate the aquifer to a depth of 17 feet below the water table. Well 1 was 24.9 feet and well 13 was 29.9 feet from the pumped well. Accordingly, if the aquifer is reasonably homogeneous areally, both hydrographs should have very nearly the same shape.

In the model-test analysis, the effect of significant water-level timelag would be to greatly increase the calculated value of S_y, as can be seen from equation 17. Because the S_y values calculated are all very much less than 0.2, it appears likely that possible errors due to timelag are relatively insignificant. In any event, the timelag for the observation wells used by Wenzel cannot be evaluated quantitatively from the data available.

According to the assumptions adopted for test analyses described, the water levels in the observation wells should have followed the idealized curve *ABC* of figure 69. The segment *AB* represents the

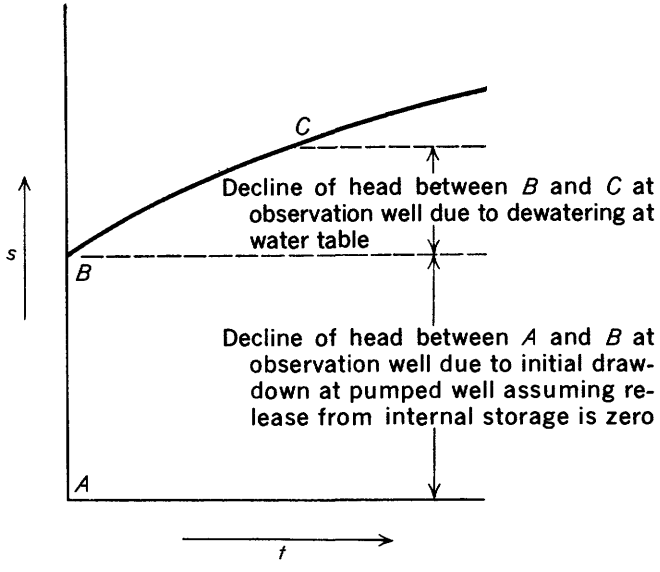

FIGURE 69.—Schematic of idealized observation well response.

initial head change due to creating an instantaneous drawdown at the pumped well. The length of *AB* is partly dependent on both the radius to, and depth of penetration, of the observation well. For an example, refer to figure 64. For well 13, $s/s_w=5\times10^{-2}$. Assuming that $s_w=20$ feet, the length of segment *AB* in a hydrograph for well 13 would be equal to $20\times5\times10^{-2}=1.0$ foot. The total drawdown observed in well 13 after 6 minutes of pumping was 1.86 feet. This latter observation was used without modification for estimating $\partial s/\partial t$ in calculation of S_y, as given in table 3. However, figure 69 shows that the correct $(\Delta s)_{t1}$ should be $1.86-1.00=0.86$ and that a better estimate of $(\Delta s)_{t1}/\Delta t_1$ would therefore be $0.86\times1{,}440/6=206.4$ feet per day. This correction applied to the data of well 13 would increase the calculated value of S_y in table 3 by a factor of about 2. For wells located at a greater distance from the pumped well or at

less depth below the water table, the AB segment of the hydrograph is a smaller proportion of the total drawdown to point C. For most of the wells listed in table 3, adjustment of the $(\Delta s)_{t1}/\Delta t_1$ values for segment AB would alter the calculated S_y values by only about 20 percent.

WATER-LEVEL CONTROL IN PUMPED WELL

In the Grand Island pumping test, the pumped well was controlled so as to maintain a virtually constant rate of pumping. Throughout the test analysis presented earlier in this report it was assumed that head was maintained constant in the pumped well throughout the period $t>0$. To what extent screen efficiency and disturbance of the aquifer materials caused by drilling affected the drawdown near the pumped well cannot be surmised. The latter effects were assumed negligible in the test analysis. Published data on water levels in the pumped well are very fragmentary. Thus it is possible only to gain a vague definition of water-level control at the pumped well.

Wenzel (1942, p. 176) listed drawdown data from two observation wells, 71 and 72, both near the pumped well (at radii of 2.6 and 12.3 ft, respectively). Neither their depths nor diameters were given. However, if it is assumed that both tapped the aquifer at such depths that the maximum initial drawdown would appear in each, it might be inferred from figures 64 and 68 that the effective drawdown at the pumped well was probably some value between 11 and 14 feet during the first 10 minutes of pumping. Also, the hydrographs from each well indicate that relatively stable heads were attained in the pumped well by the time pumping extended more than 4 minutes. This interpretation, however, does not preclude entirely the possibility that the effective drawdown was greater than 14 feet.

Although the discharge at the pumped well was controlled, the drawdown evidently became nearly constant just a few minutes after pumping began. The assumed initial conditions relating to drawdown control are therefore defined satisfactorily for the model analysis undertaken. However, the value of s_w for calculating permeability is in question, and it cannot be resolved with accuracy from the data available. Permeability values calculated are directly proportional with the assumed s_w, but values of S_y calculated by means of equation 17 are unaffected by the assumed value of s_w.

MODEL ADAPTED FOR ANALYSIS OF NONSTEADY FLOW

Pumping-test analysis described in the foregoing sections of this report has been based on the concept that, for a short period of time after pumping begins, the flow system may be treated as being in the steady state. The difficulty of adequately controlling either the draw-

down or the discharge rate at the pumped well and questionable response characteristics of observation wells during the first few minutes of pumping lead to gross uncertainties in the data and their application to aquifer analysis. Although there are advantages to the shorter testing period and the steady-state analysis, where control and response are inadequate, the total testing time must be extended from a few minutes to several hours. As was demonstrated earlier, even after several hours of pumping at the Grand Island site, vertical-flow components were still controlling the downward movement of the water table. Also, Boulton's criteria suggest that changes in potential along the water table need to be considered in constructing the flow system as a function of time for test periods several hours in duration.

For as long a period as equation 13 remains an adequate approximation of the flow conditions at the water table, the flow system in nonsteady state form may be modeled easily, assuming that specific yield is constant with time. The nonsteady state model may be developed directly from the resistance grid already defined, adding electrical capacity to account analogically for the storage characteristics of the aquifer.

An array of nodes near the water table and its equivalent in the resistance grid are shown on figure 70. The capacitor, C_{WT}, represents

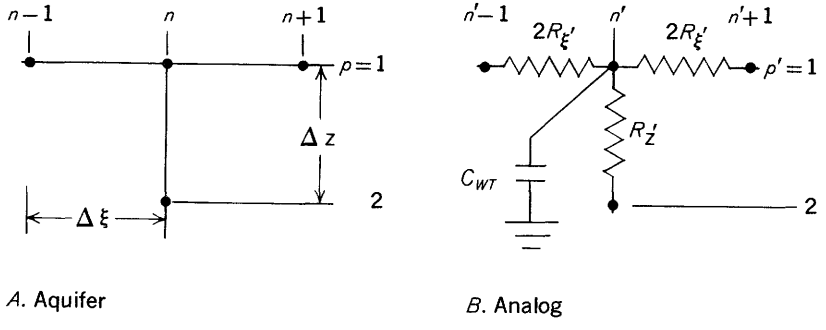

FIGURE 70.—Analogic relations at water table for nonsteady flow. *A*, Aquifer; *B*, Analog.

the electrical storage equivalent of S_y. For electrical flow to the junction ($p'=1$, n'), where radial-flow components are comparatively small, current flow to the junction may be expressed in the following form:

$$R_{z'}C_{WT}\frac{\partial e_{(p'=1,\,n')}}{\partial t'}=-(e_{p'=1}-e_{p'=2})_{n'}, \qquad (19)$$

where t' represents elapsed time on the model, and the subscript notation is defined by figure 70*B*.

The flow conditions in the vicinity of the corresponding point ($p=1$, n) in the aquifer can be derived from equation 13, from which:

$$\frac{\Delta z S_y}{P_z}\frac{\partial s}{\partial t}=-(s_{p=1}-s_{p=2})_n. \tag{20}$$

Comparison of equations 19 and 20 provides the relations between aquifer and electrical storage required for model scaling. It will be convenient to define two scaling constants for this purpose. One, the proportionality between voltage and drawdown has already been discussed. It may be defined as

$$s/e=K_{es}. \tag{21}$$

The other, relating the aquifer prototype time, t, to time on the model, t', may be stated as

$$t/t'=K_t. \tag{22}$$

By differentiating equation 22, it is easily shown that

$$K_t\frac{\partial t'}{\partial t}=1. \tag{23}$$

Substituting for s in equation 20, its equivalent expression as given by equation 21 yields

$$\frac{\Delta z S_y}{P_z}\frac{\partial e_{(p'=1,\ n')}}{\partial t}=-(e_{p'=1}-e_{p'=2})_{n'}, \tag{24}$$

and multiplying the left side of equation 19 by equation 23 yields

$$K_t R_{z'} C_{WT}\frac{\partial e_{(p'=1,\ n')}}{\partial t}=-(e_{p'=1}-e_{p'=2})_{n'}. \tag{25}$$

Equating 24 and 25, and solving for C_{WT}, gives the relation

$$C_{WT}=\frac{\Delta z S_y}{P_z K_t R_{z'}}\ \text{farads}. \tag{26}$$

Equation 26 is the final relation sought for determining the analogic storage characteristics at each point ($p'=1, n'$) on the model. Within limitations of electronic instrumentation and measurement, the distribution of values of C_{WT} may be selected inversely proportional to $R_{z'}$ at each node of the resistance grid. The time constant, K_t, is then determined by the ratio $\Delta z S_y/P_z$, which can be found independently by test analysis.

Data from the Grand Island test site might be used to obtain a measure of a practical K_t value to be expected. For this aquifer system, use of $S_y=0.2$ and $P_z=100$ feet per day (the latter is a fictional value) and $C_{WT}=1{,}000$ microfarads at $R_{z'}=0.2$ ohm, with $\Delta z=5$ feet, results in

$$K_t=\frac{5\times 0.2}{1\times 10^2\times 1\times 10^{-3}\times 0.2}=50.$$

Thus each second on the analog represents 50 seconds of pumping time for the conditions assumed.

The release of internal storage might be modeled in similar fashion, where the effects from such storage on water-level changes are significant. The equation describing the drawdown interrelations at interior points of the flow field may be taken from equation 3 and written in finite-difference form as follows:

$$s_{n+1}+s_{n-1}-2s_n+\left(\frac{r_n\Delta\xi}{\Delta z}\right)^2\frac{P_z}{P_r}(s_{p+1}+s_{p-1}-2s_p)=(r_n\Delta\xi)^2\frac{S'}{P_r}\frac{\partial s}{\partial t}. \quad (27)$$

The array of grid intersections at which equation 27 applies is shown on figure 71*A*.

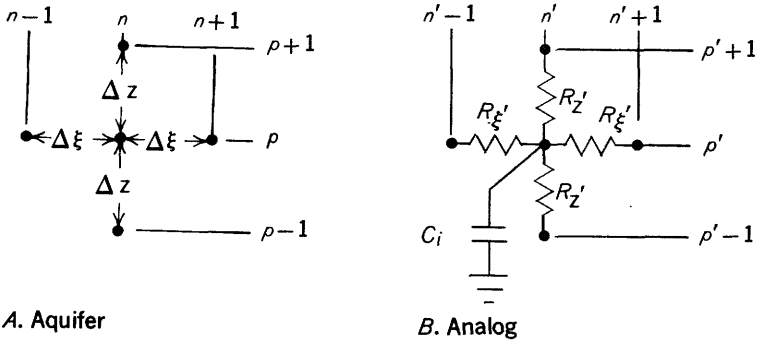

FIGURE 71.—Analogic relations at interior points for nonsteady flow. *A*, Aquifer; *B*, Analog.

The corresponding array on the analog is shown on figure 71*B*, for which it can be shown that

$$e_{n'+1}+e_{n'-1}-2e_{n'}+\frac{R_{\xi'}}{R_{z'}}(e_{p'+1}+e_{p'-1}-2e_{p'})=R_\xi C_i\frac{\partial e}{\partial t'}. \quad (28)$$

Making use of equations 12, 21, 22, and 23 in equations 27 and 28, it can be shown that

$$C_i=\frac{(\Delta z)^2S'}{K_tR_{z'}P_z}\text{ farads}. \quad (29)$$

To provide a homogeneous model with respect to time scaling, the value of K_i in equation 29 must be the same as its value in equation 26. Thus at each value of ξ' in the model the relation between C_i and C_{WT} is

$$C_i=\frac{\Delta z S'}{S_y}C_{WT}, \tag{30}$$

as may be found by dividing equation 29 by equation 26. By again using the Grand Island test data for an example, where $C_{WT}=1\times10^{-3}$ farads, $S_y=0.2$, $\Delta z=5$ feet, and $S'=5.4\times10^{-7}$, it is seen that

$$C_i=\frac{5\times5.4\times10^{-7}}{0.2}\times1\times10^{-3}=1.35\times10^{-8}=0.0135 \text{ microfarad.}$$

According to equations 29 and 30, C_{WT} and C_i are inversely proportional to $R_{z'}$. C_{WT} was assigned a value of 1×10^{-3} farads at $R_{z'}=0.2$. All other $R_{z'}$ values are larger than 0.2, and therefore all capacitors in the model will be smaller than 1×10^{-3} farads. Similarly, the internal capacitors would all be less than 0.0135 microfarad as each is inversely proportional to $R_{z'}$. Thus at $n=3$, for example,

$$C_{WT}=\frac{1\times10^{-3}\times0.2}{7.14\times10^{6}}=28 \text{ micromicrofarads}$$

and

$$C_i=\frac{1.35\times10^{-8}\times0.2}{7.14\times10^{6}}=3.8\times10^{-16} \text{ farads}$$

$$=3.8\times10^{-4} \text{ micromicrofarads.}$$

The latter value of C_i is probably much less than the capacity of the wire leads and resistance elements, and therefore it would be impossible to model internal storage accurately at the smaller radii without modification of the analog design from that already stated. The analog designer enjoys a certain amount of latitude for gaining the proper balance between component selection, test equipment, and prototype flow conditions. For this report, the fundamental equations that may be used as the basis for analog design are presented only in general terms. From them, analog grids may be designed to fit the particular flow system to be investigated.

Analogic treatment of nonsteady flow may require that the aquifer be modeled beyond the radius adopted in the resistance grid described earlier. This requirement did not arise in the example solutions, because flow components from regions of large $\frac{r}{m}$ value were negligible; but it may arise for nonsteady flow analysis, because contributions

from storage at large values of r/m become increasingly significant to the drawdown distribution as time increases. The example resistance grid was terminated, as indicated on figure 62, at $\frac{P_r}{P_z}\frac{r}{m}=49.4$ because of limitations in low-cost resistor availability. In order to remain within these limitations, the model may be extended, if required, by changing the value of $\Delta\xi$ to a smaller value at and beyond one of the larger radii. This would permit the use of higher-valued $R_{z'}$ components of lower cost at the larger radii but would require more of them to simulate a given radial distance. For study of nonsteady flow such a design procedure would also reduce the C_{WT} values and thereby decrease unit cost, but it would also require installation of more units. Extending the grid in this way is similar to the use of "graded nets" as described by Southwell (1946) and is frequently employed in numerical analysis.

SUMMARY OF RESULTS

Design features of an electric analog of flow to wells in unconfined aquifers, including vertical-flow components, were derived from the basic differential equations of ground-water motion. The analog relations developed were applied to construct a resistance grid that was used for computing permeability and specific yield from the Grand Island pumping-test data of Wenzel (1936, 1942). The method of analysis used followed that of Boulton (1954), in which the form of drawdown distribution is assumed to be virtually constant for a short period of time after pumping begins.

Numerical results from the model studies show that permeability and specific-yield estimates are highly dependent on the flow conditions assumed to exist in the aquifer. Specific-yield estimates seem much more sensitive to variations in assumed-flow conditions, such as degree of penetration of the pumped well, nonhomogeneity, and anisotropy, than are the estimates of permeability to flow along horizontal planes as obtained by model studies. Adequate pumping-test analysis by electrical models requires that the degree of anisotropy and nonhomogeneity be known independently of model analysis. A procedure for observing anisotropy relations directly in the field is suggested, for which a minimum of five observation points is required, all located in a prescribed pattern. Sufficient drawdown observations should be made near the water-table position to provide detailed hydrographs at observation wells and the pumped well for at least 15 minutes after pumping begins. For the steady-state type of test analysis described, the pumped well should be operated at constant drawdown. For tests of short duration, the well array for measuring anisotropy and observation wells for the model analysis should

ordinarily be located at distances from the pumped well in the range of approximately 0.1 and 1.0 times the aquifer thickness.

Use of test data from pumping periods of only a few minutes in duration provides for good definition of the aquifer characteristics regulating vertical flow. However, as a prerequisite to electric-model analysis of such data, special pressure measuring devices with rapid response characteristics may be needed in place of comparatively slow-response observation wells.

Numerical investigations of the drawdown data collected by Wenzel (1936, 1942) near Grand Island, Nebr., show that vertical-flow components were predominantly responsible for regulating the rate of change of the water-table position several hours after pumping began and that specific yield was probably of the order of 0.01 during the first few minutes of pumping. This result serves to emphasize the futility of calculating permeability and specific yield from analytical expressions in which vertical flow components are assumed to be negligible and specific yield is assumed to be constant from pumping tests of short duration in unconfined systems.

REFERENCES

Birch, Francis, ed., 1942, Handbook of physical constants: Geol. Soc. America Spec. Paper 36.

Boulton, N. S., 1951, The flow pattern near a gravity well in a uniform water-bearing medium: Jour. Inst. Civil Engineers (British), p. 534–550.

——— 1954, The drawdown of the water table under non-steady conditions near a pumped well in an unconfined formation: Proc. Inst. Civil Engineers (British), p. 564–579.

Dorsey, N. E., 1940, Properties of ordinary water substance: New York, Reinhold Publishing Corp.

Ferris, J. G., 1949, Ground water, Chapter 7 *in* C. O. Wisler and E. F. Brater, Hydrology: New York, John Wiley and Sons.

Ferris, J. G., Knowles, D. B., Brown, R. H., and Stallman, R. W., 1962, Theory of aquifer tests: A summary of lectures: U.S. Geol. Survey Water-Supply Paper 1536–E, p. 69–174 (in press).

Jacob, C. E., 1950, Flow of ground water, Chapter 5 *in* Hunter Rouse, Engineering Hydraulics: New York, John Wiley and Sons.

Kirkham, Don, 1959, Exact theory of flow into a partially penetrating well: Jour. Geophys. Research, v. 64, p. 1317–1327.

Southwell, R. V., 1946, Relaxation methods in theoretical physics: London, Oxford Univ. Press.

Theis, C. V., 1935, The relation between the lowering of the piezometric surface and the rate and duration of discharge of a well using ground-water storage: Am. Geophys. Union Trans., p. 519–524.

Wenzel, L. K., 1936, The Thiem method for determining permeability of water-bearing materials: U.S. Geol. Survey Water-Supply Paper 679–A.

——— 1942, Methods for determining permeability of water-bearing materials: U.S. Geol. Survey Water-Supply Paper 887.

○